Photoinduced Conductivity of a Porphyrin−Gold Composite Nanowire†

Dmitri S. Kilin,‡ Kiril L. Tsemekhman,§ Svetlana V. Kilina,|| Alexander V. Balatsky,|| and Oleg V. Prezhdo*,§

Quantum Theory Project, Departments of Chemistry and Physics, University of Florida, Gainesville Florida 32611-8435, Department of Chemistry, University of Washington, Seattle Washington 98195-1700, and T-Division and Center for Integrated Nanotechnologies (CINT), Los Alamos National Laboratory, Los Alamos, New Mexico 87545

Received: December 18, 2008; Revised Manuscript Received: February 3, 2009

Negatively charged phosphine groups on the backbone of DNA are known to attract gold nanoclusters from a colloid, assembling the clusters at fixed intervals. Bridging these intervals with porphyrin−dye linkers forms an infinite conducting chain, a quantum wire whose carrier mobility can be enhanced by photoexcitation. The resulting nanoassembly can be used as a gate: a wire with a controllable conductivity. The electronic structure of the porphyrin−gold wire is studied here by density functional theory, and the conductivity of the system is determined as a function of the photoexcitation energy. Photoexcitations of the dye are found to enhance the wire conductivity by orders of magnitude.

I. Introduction

Self-assembly and patterning of matter on the nanometer scale is an actively pursued goal of modern chemistry and physics of materials.[1−4] The studies are motivated by the need to further miniaturize the components of electronic, optical, and other types of devices. Additional advantages are provided by the strong size-dependence of material properties on the nanometer scale, allowing one to tune the desired characteristics with high precision and sensitivity.[5] Chemical, electronic, magnetic, and optical behavior of nanometer size crystals in particular are governed by quantum confinement and surface effects.[6,7] "Top-down" methods, such as lithography, can reach only to the upper limit of the nanometer regime.[8] At the same time, "bottom-up" wet chemistry techniques provide a means for preparation of monodisperse, defect-free crystallites just 1−10 nm in size.[9,10] Generation of assemblies of such nanocrystals with molecular and biological components and accurate control of their structure constitutes the next challenge.

More than ten years ago it was first shown that DNA oligonucleotides can be attached to gold nanoparticles rationally to direct the formation of larger assemblies.[1,11] Over the past decade, the functionalized particles were used to develop nucleic acid and protein detection tools,[12] intracellular probes,[13] and gene regulators.[14] At the same time, the conceptually simple idea of rational assembly of nanoparticles through controlled DNA interactions into ordered macroscopic materials has not yet been fully realized. In spite of the significant progress in the assembly of large patterns, they remain primarily nonelectronic in their properties.[15,16] The control over the placement and distance between particles within the assembled polymeric materials remains modest. Further progress in the understanding of the fundamental principles of self-assembly and improvement of the material design requires theoretical modeling in close connection with experiments.[17−21]

In this paper we consider elements for molecular electronics and computing that can be created by DNA-templating. Nanolithography, widely used in modern microchip production, cannot be applied on the scale of individual molecules and clusters. The molecular scale calls for chemical self-assembly.[22−24] DNA templates can provide an outstanding basis for the molecular technology. The DNA backbone includes PO_4 groups, which carry negative charge and can form coordination bonds with nanoscale elements of electronic circuits. In particular, the DNA backbone can directly, or through a bridge, bind to gold clusters.[25−27] Arrangement of gold clusters at fixed distances from each other is one of the most attractive features of such an assembly. The spaces between the gold clusters can be occupied by linkers, creating infinite chains or quantum wires.[28] Such wires can be used to permanently conduct electricity.

Alternatively, self-assembled DNA−gold-linker nanowires can be designed as programmable gate elements, whose conductivity is controlled from the outside. The electronic structure of the linkers in a programmable wire should differ from that of the gold clusters. Then, an outside source can control linker properties without affecting the nanoparticles. One prospective design uses porphyrin dyes to link the clusters.[29,30] This choice offers two advantages. First, we consider an infinite chain of 38-atom gold clusters bridged by porphyrin molecules with its spatial period corresponding to the spatial period of the B-form of DNA. Second, the lowest energy electronic excitation of porphyrin is around 2 eV. As a result, porphyrin is an insulator when in the ground state. In contrast, photoexcited porphyrins transport charge and energy in many biological systems. Excitation of porphyrin linkers facilitates carrier mobility along nanowires.[31] Integration of these novel techniques with the traditional printed circuitry is under development.[32]

This paper presents an ab initio analysis of the nanowire composed of Au_{38} clusters linked by porphyrins. An atomistic model is used to compute the photoinduced conductivity of the wire in response to a periodic electric field for different photoexcitation energies. The paper is constructed as follows. The next section outlines the density functional theory (DFT) used to describe the electronic structure of the system. Then,

† Part of the "George C. Schatz Festschrift".

* Corresponding author. E-mail: prezhdo@u.washington.edu.
‡ University of Florida.
§ University of Washington.
|| Los Alamos National Laboratory.

10.1021/jp811169c CCC: $40.75
Published on Web 03/11/2009

the formalism for calculating the conductance of the nanowire under irradiation by light is presented. Following a description of the computational details, the Results and Discussion section investigates the conductance of the wire as a function of the electric field frequency and voltage for different photoexcitation energies. The conductivity mechanism for each case is analyzed in detail at the atomistic level. The paper concludes with a summary of the key findings.

II. Electronic Structure Calculations with Density Functional Theory

The electronic structure of the porphyrin−gold nanowire is computed by using DFT, which provides a practical approach for describing large interacting many-particle systems and can be utilized to describe transport properties.[33−36] According to ref 37, application of the density-based variational principle to the many-body electronic energy is operationally equivalent to solving a set of coupled single-particle equations, known as the Kohn−Sham (KS) equations. Here, DFT makes contact with the Schrödinger description, and the KS theory links DFT to an orbital picture. The total energy functional includes the electron kinetic energy, the electrostatic electron−electron repulsion, the interaction of electrons with the atomic nuclei, and a purely quantum-mechanical contribution comprising the exchange and correlation effects. The latter is known as the exchange-correlation functional and includes the difference between the exact kinetic energy and the kinetic energy of noninteracting particles.[38,39] The KS theory maps the interacting many-electron system onto the equal number of noninteracting electrons interacting with a properly chosen effective one-electron potential $v_s(\mathbf{r})$. The single-particle equations for the KS orbitals $\phi_i(r)$, $i = 1, 2,..., N$, are

$$\{-\nabla^2/2 + v_s(r)\}\phi_i(r) = \varepsilon_i\phi_i(r) \quad (1)$$

The effective potential $v_s(\mathbf{r})$ includes the Hartree theory terms and a term representing the quantum-mechanical exchange-correlation effects. The sum of the squares of the occupied KS orbitals $\sum_{i\leq \mathrm{HOMO}}|\phi_i|^2$ yields the ground state electron density of the system. The energies of the highest occupied molecular orbital (HOMO) and the lowest unoccupied molecular orbital (LUMO) are related to the ionization potential and electronegativity.[40,41]

The KS orbital picture can be used for analysis of electronic excitations. The linear response formulation of the time-dependent (TD) DFT gives a rigorous description of the system's response to a weak perturbation.[42] The perturbation is weak in the sense that it does not destroy the ground state structure of the system. In this spirit, weak low-energy excitations of large systems, such as the nanowire, introduce only small changes to the ground state density, and the difference between the KS eigenvalues calculated by using the ground state density can serve as a reasonable approximation to a more rigorous TDDFT excitation energy.[43] The KS approximation[44−46] and constrained DFT[47−49] generate a good description of optical transitions of porphyrins and are in reasonable agreement with each other and experiment. Similarly, as shown in ref 50 transition energies between the KS orbitals of the DNA bases are in reasonable agreement with the excitation energies calculated by TDDFT with various functionals. Further, excited states of metallic clusters rapidly relax to the ground state. All-in-all, subjected to a weak continuous radiation and applied voltage, the molecular wire approaches a steady state, in which the charge density differs little from that of the ground state. Alternative and computationally more demanding methods for calculating steady-state densities within DFT can be found in refs 44, 51, and 52.

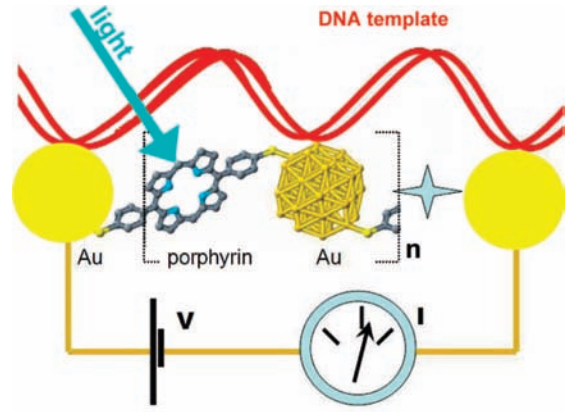

Figure 1. Schematic of the studied model. The red line represents the double-strand of the DNA template. The molecular structure of a unit cell of the porphyrin−gold nanowire is enclosed in rectangular brackets to emphasize the periodic character of the nanowire. Hydrogen atoms are not shown. Leads, applied external voltage, and electric current through the nanowire are shown in the lower portion of the scheme. Optical excitation of the nanowire is symbolized by the blue arrow.

DFT provides an efficient tool for modeling quantum transport on atomic, molecular, and nanometer scales.[53] Conductivity of periodic, homogeneous materials can be calculated semiclassically, taking advantage of small variations in the electron distribution function.[54,55] Within the linear response approach, the real part of the conductance can be calculated based on the Kubo−Greenwood formula.[56−59] Conduction of molecular junctions[60] is often modeled based on the quantum scattering formalism, including the well-known generalized Landauer expression.[61] Models based on the Landauer theory give good results in agreement with experiments.[62] The nonequilibrium Green's function (NEGF) technique[63] provides a more advanced treatment and naturally includes contributions from both scattering and bound states. DFT implementations of the NEGF theory are instrumental in modeling of the quantum transport in molecular electronic devices.[64,65] The NEGF-DFT method is particularly well suited for studies of finite size molecular junctions, such as dithiol and porphyrin dithiolate,[60,66] that are placed between gold electrodes.[67,68] It is important for the present system, Figure 1, that variations in the mutual geometries of thiol groups and gold leads do not significantly influence conductance through the junction.[62]

III. Calculation of the Optical Spectrum and Photoinduced Conductivity of the Nanowire

In the plane-wave DFT implementation to spatially periodic systems, the KS orbitals are expanded in the plane wave basis as

$$\phi_j(\mathbf{r}) = \sum_{|\mathbf{G}|<\mathbf{G}_{\mathrm{cutoff}}} C_{j,\mathbf{G}} \exp\{-i\mathbf{G}r\} \quad (2)$$

The three-dimensional vectors $\mathbf{G}$ are the reciprocal lattice vectors, and the vector $\mathbf{G}_{\mathrm{cuttoff}}$ determines the cutoff for the basis-set expansion. The coefficients $C_{j,\mathbf{G}}$ define the KS orbitals in the momentum representation.[46,69,70] Typically, $\phi_j(\mathbf{r})$ are defined in a supercell that is periodic in all three dimensions. In the

current case of a one-dimensional system extended in the *Z*-direction, the artificial periodic images in the *X*- and *Y*-directions are separated by vacuum in order to reduce the spurious interaction between the images. The images are connected in the *Z*-direction, forming a one-dimensional periodic crystal.

The transition operator $\mathbf{D} = \sum_{ij}|i\rangle\,\mathbf{D}_{ij}\langle j|$ is obtained from the optical transition matrix elements calculated according to the formula[46,70]

$$\mathbf{D}_{ij} = \langle i|\hat{\mathbf{D}}|j\rangle = \sum_{\mathbf{G},|\mathbf{G}'|<\mathbf{G}_{\text{cuttoff}}} C^*_{i,\mathbf{G}}\mathbf{D}_{\mathbf{G},\mathbf{G}'}C_{j,\mathbf{G}'} \qquad (3)$$

where $\hat{\mathbf{D}}$ is the dipole moment operator.

The density of states for a continuous energy spectrum is given by the following expression in the KS representation

$$n(\varepsilon) = \sum_j \frac{1}{\sqrt{2\pi\gamma}} \exp\{-(\varepsilon_j - \varepsilon)^2/\gamma^2\} \qquad (4)$$

where ε_j are the KS energies and γ is a smearing parameter.

In the continuous band limit, the absorption spectrum can be expressed as

$$\alpha(\Omega) = \frac{1}{\hbar\Omega}\int_{-\infty}^{\infty} d\varepsilon |D_{\varepsilon,\varepsilon+\Omega}|^2 n(\varepsilon) f_0(\varepsilon)\bar{n}(\varepsilon+\Omega)\bar{f}_0(\varepsilon+\Omega) \qquad (5)$$

where f_0 represents the distribution of electron occupation numbers for the ground state, while $\bar{n}$ and $\bar{f}_0$ denote the corresponding quantities for holes.

In the limit of discrete orbitals, the absorption spectrum reads

$$\alpha(\Omega) = \sum_{i\le \text{HOMO}} \sum_{j>\text{LUMO}} |D_{ij}|^2 \frac{1}{\sqrt{2\pi\gamma_{ij}}} \exp\{-(\varepsilon_j - \varepsilon_i - \hbar\Omega)^2/\gamma_{ij}^2\} \qquad (6)$$

This expression is used to compute the optical spectra reported below. It is assumed that each transition has the broadening $\gamma_{ij} = \gamma$. The broadening is induced primarily by dephasing interactions[71] with vibrations of the porphyrin and the metal cluster.[72]

Under continuous excitation with light of frequency Ω, accompanied by relaxation and recombination, the electronic system reaches a steady state. The change of the occupation numbers is proportional to the square of the matrix element of the transition operator

$$\text{for holes, } \varepsilon < \varepsilon_{\text{Fermi}}: f_\Omega(\varepsilon) \propto f_0(\varepsilon) - |D_{\varepsilon,\varepsilon+\Omega}|^2 \bar{n}(\varepsilon)\bar{f}_0(\varepsilon) n(\varepsilon+\Omega) f_0(\varepsilon+\Omega)$$
$$\text{for electrons, } \varepsilon > \varepsilon_{\text{Fermi}}: f_\Omega(\varepsilon) \propto f_0(\varepsilon) + |D_{\varepsilon-\Omega,\varepsilon}|^2 \bar{n}(\varepsilon-\Omega)\bar{f}_0(\varepsilon-\Omega) n(\varepsilon) f_0(\varepsilon) \qquad (7)$$

The increment is proportional to the probability of electron excitation from the valence band (VB) to the conduction band (CB). A derivation of the distribution of steady-state populations can be found in ref 70. For a sparse spectrum the population distribution $f_\Omega(\varepsilon)$ can be approximated by promoting an electron between those pairs of orbitals i, j that match the resonance condition $(\varepsilon_j - \varepsilon_i) \rightarrow \hbar\Omega$.

An electric field of frequency ω, voltage V per unit chain length Δz, and strength $E_z = V/\Delta z$ applied along the wire induces an electric current characterized by the current density $J_z = \sigma_{zz}(\omega)E_z(\omega)$. Generally, the current density in the ith direction equals $J_i = \sum_j \sigma_{ij}(\omega)E_j(\omega)$. Here, we consider only the $\sigma_{zz}(\omega)$ component of conductance and, for simplicity, denote it as $\sigma(\omega)$. In the weak field limit the conductivity is[57,59]

$$\sigma(\omega) = \frac{1}{\hbar\omega}\int_{-\infty}^{\infty} d\varepsilon \langle\varepsilon|\hat{j}|\varepsilon+\omega\rangle\, n(\varepsilon) f_\Omega(\varepsilon)\,\bar{n}(\varepsilon+\omega)\,\bar{f}_\Omega(\varepsilon+\omega) \qquad (8)$$

The bra and ket vectors $\langle\varepsilon|$, $|\varepsilon+\omega\rangle$ represent the states of electron and hole. $\langle\varepsilon|\hat{j}|\varepsilon+\omega\rangle$ is the matrix element of the current operator that is expressed in terms of the carrier momentum in the direction of transport. The densities of states and the occupation numbers of holes and electrons are related by $\bar{n}(\varepsilon) = n(\varepsilon)$, $\bar{f}(\varepsilon) = 1 - f(\varepsilon)$. Transition from the continuous band limit to a discrete state representation is performed in the same fashion as for $\alpha(\Omega)$, eq 6.

Equation 8 leads to the following conditions that should be satisfied by pairs of electron and hole states in order to promote conductivity. (i) The matrix element of the current operator between a given pair of states, $\langle\hat{j}\rangle$, cannot vanish. To satisfy this condition, the states should overlap and have proper symmetries. (ii) The densities of states of electrons and holes, n and $\bar{n}$, should be large at the relevant energies. (iii) The initial state should be occupied by an electron, $f(\varepsilon) \approx 1$, and the final state should be occupied by a hole, i.e., empty of an electron, $\bar{f}(\varepsilon) \approx 1$. (iv) The energy difference between the electron and hole states should match the field frequency ω.

Examination of the porphyrin−gold nanowire in view of the above criteria leads to the following observations. The low-energy states are localized either on the dye or on the quantum dot. Therefore, for the current to flow, the matrix elements of the current operator should involve electron and hole states that are localized on different species. If the wire is in the ground electronic state, the occupation numbers are such that the available electron and hole states are far from each other in energy, and this diminishes the overall conductivity. The conductivity can be increased by changing the occupation numbers through doping, charge injection, or electronic excitation. Here, we consider the excitation process, since porphyrin is an efficient light absorber. The photoexcitation will modify the occupation numbers from $f_0(\varepsilon)$ to $f_\Omega(\varepsilon)$, eq 7, populate electron and holes states of similar energies, and, thereby, create new channels for electric current.

IV. Computational Details

An atomic model of a heterogeneous quantum wire is presented in Figure 1. Each porphyrin molecule was connected to a gold cluster through benzene-ring spacers containing thiol groups. The shape of the 38-atom gold cluster was roughly spherical. The size of the gold cluster as well as the orientation and positions of the cluster−porphyrin coordination bonds were chosen to match the period of DNA. The geometry of an oligomer of four repeating $-(H_2P-Au_{38})-$ units was optimized by using a classical-mechanical force field, see Supporting Information. A single repeating unit was extracted from this oligomer, and its geometry was optimized further with DFT by using periodic boundary conditions, see Supporting Information.

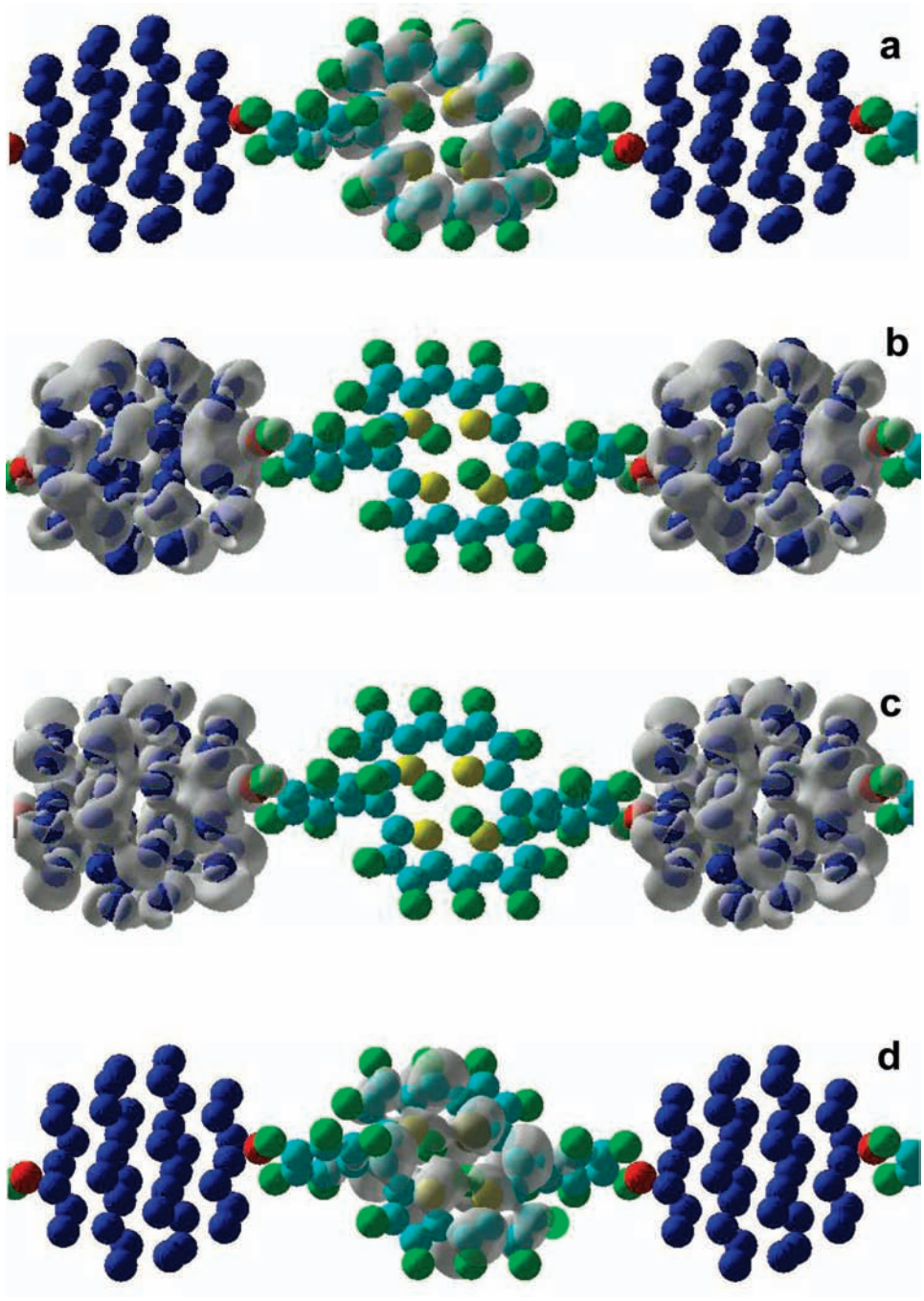

Figure 2. Densities (gray clouds) for the Kohn−Sham orbitals of the composite nanowire contributing to the photoinduced conductivity at the lowest excitation energy: (a) $LUMO_{H_2P}$, (b) $(LUMO+9)_{Au_{38}}$, (c) $(HOMO-2)_{Au_{38}}$, and (d) $HOMO_{H_2P}$. Atoms are color coded as follows: H (green), C (cyan), N (yellow), S (red), Au (blue). All charge densities are substantially localized on one or the other species forming the nanowire. The overlap of the exponentially decaying edges of the orbitals in the contact region between the species is responsible for charge conductance along the wire.

The period in the *Z*-direction equaled $\Delta z = 16.1049$ Å. Upon geometry optimization, the conductivity of the composite nanowire was studied in the longitudinal direction.

The DFT electronic structure calculations were performed using the VASP code.[73] It is well suited for studies of large periodic systems. A vacuum layer of at least 7 Å was added along the two directions perpendicular to the wire, in order to avoid spurious interactions between periodic images of the system. The core electrons were modeled by using the Vanderbilt pseudopotentials.[74] The valence electrons were treated explicitly with a converged basis set of roughly 10^6 plane waves. The PW91 generalized gradient approximation was employed to account for the electron exchange and correlation effects.[75] The electronic structure was converged to the 0.0001 eV tolerance limit providing the total energy of −486.0976 eV per simulation cell.

V. Results and Discussion

The conductivity of the porphyrin−gold nanowire is determined by the energies and localizations of the KS orbitals. Figure 2 shows the charge densities of four representative orbitals. Typically, the orbitals are substantially localized on one or the other subsystem. Parts a and d depict the LUMO

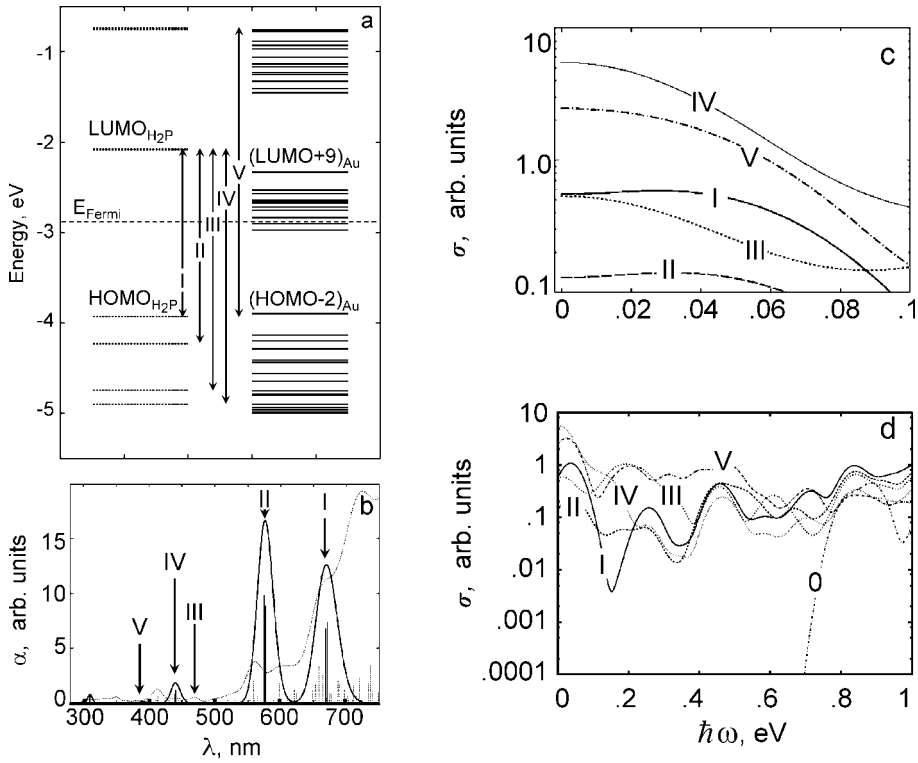

Figure 3. Electronic properties of the composite nanowire. (a) Energies of the Kohn−Sham orbitals localized on porphyrin (left, dashes) and Au_{38}-cluster (right, solid lines). Optical transitions within porphyrin are indicated with arrows and are labeled by Roman numbers I, II, III, IV, V, according to increasing transition frequency. (b) Absorption spectra of porphyrin (solid lines) and gold-cluster (dashes). Peaks I and II correspond to the Q-band of porphyrin, while III, IV, and V correspond to the Soret band. (c and d) Photoinduced AC-conductance of the composite nanowire as a function of energy $\hbar\omega$ corresponding to AC-frequency ω. 0.01 eV gives 2.418 THz. Parts c and d show the same data at different $\hbar\omega$ scales. The lines are labeled by Roman numbers according to the excited transition, see parts a and b. Line 0 gives ground state conductance.

and HOMO of the porphyrin molecule, while parts b and c show the gold cluster orbitals that are closest in energy to the LUMO and HOMO of the porphyrin. The energies of these orbitals are given in Figure 3a. Since gold is a metal, the energy gap between the HOMO and LUMO of the gold cluster is small; however, the gap between HOMO-1 and HOMO-2 is largely due to spatial confinement. Similarly, there is a finite gap between LUMO+9 and LUMO+10 of the gold cluster. The LUMO and LUMO+1 orbitals of the porphyrin molecule are doubly degenerate because of the symmetry of the porphyrin dye. The wire conductivity depends strongly on the relative energies of the orbitals localized on the molecule and the cluster. Figure 3a suggests that the gold−porphyrin nanowire more readily supports hole conductivity, because a number of porphyrin orbitals below the Fermi energy are in near resonance with the VB orbitals of the gold cluster.

The absorption spectrum of the gold−porphyrin nanowire is shown in Figure 3b. The location and heights of the vertical lines represent transition energies and oscillator strengths, respectively. The optical transitions associated separately with the cluster and the molecule can be easily identified based on their orbital origin, Figure 3b. The gold cluster absorbs essentially at all wavelengths (dashed lines). The spectrum of the porphyrin molecule exhibits distinct bands labeled by Roman numbers (solid lines). Peaks I and II correspond to the Q-band of porphyrin, while peaks III, IV, and V correspond to the Soret band.[76] The vertical lines obtained from the calculations were broadened according to eq 6 with $\gamma = 0.1$ eV representing a number of broadening factors, including vibrational dephasing, Franck−Condon progression, etc. The calculated intensity of the Soret band is lower than in experiment[76] due to the approximate description of the photoexcitations. As expected, the gold cluster has fewer transitions in the visible region than in the infrared region, and these transitions are less intense.[77] The porphyrin excitations are particularly important for the wire conductivity. Gold is a metal and conducts well in the ground state. On the other hand, the molecule is an insulator and must be excited to support charge transport. Transition I of the porphyrin overlaps strongly with the cluster transitions. Transition II is most intense. Transitions III and V are barely visible. Transition IV gives the highest conductivity, Figure 3c, because it creates a hole in the porphyrin orbital that is close in energy to a number of the orbitals of the gold cluster, as shown in Figure 3a.

Panels c and d of Figure 3 present the conductivity of the nanowire as a function of the frequency of the alternating current (AC) for different excitations of the porphyrin, I through V, eq 8. The energy scale of the x-axis $\hbar\omega$ corresponds to the AC-frequency ω. In particular, 0.01 eV corresponds to 2.418 THz. Part d shows the same data over a broader energy range, and includes conductivity for porphyrin's ground state 0. The conductivity at zero frequency describes direct current (DC). The dependence of the conductivity on the AC frequency varies for different photoexcitations of the porphyrin molecule, depending on the properties of the KS orbitals involved in these excitations. Particularly important are the quantity of orbitals at the relevant energies and the orbital overlaps, see discussion following eq 8. The best conductivity of the wire is generated by transition IV, which is part of the Soret band. Transition I deserves attention as well. The lowest energy transition, it provides good conductivity compared, for instance, to the second lowest transition II.

Analysis of the orbital origin of the porphyrin photoexcitations, Figure 3a, allows us to conclude that the conductivity

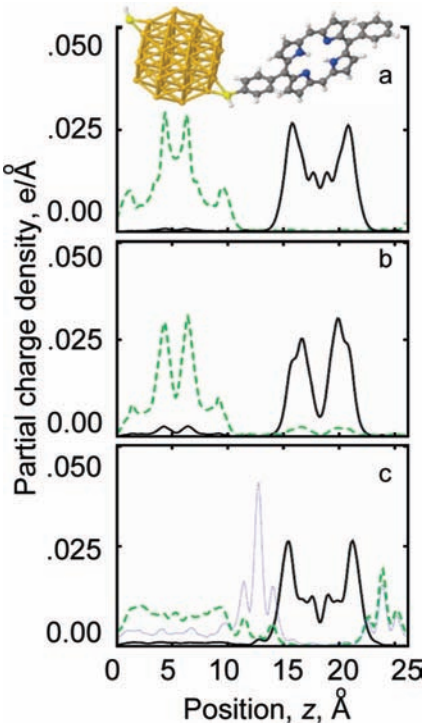

Figure 4. Analysis of overlap of the Kohn−Sham orbitals involved in electron transport for various optical excitations. (a) Excitation II induces hole transfer mediated by $(HOMO-1)_{H_2P}$ (green dashes) and $(HOMO-4)_{Au_{38}}$ (solid line). (b) Excitation IV induces hole transfer mediated by $(HOMO-3)_{H_2P}$ (green dashes) and $(HOMO-13)_{Au_{38}}$ (solid line). (c) Excitation V induces electron transfer mediated by the orbital of the bridging benzene (blue dotted line), $(LUMO+1)_{H_2P}$ (green dashes), and $(LUMO+23)_{Au_{38}}$ (solid line). The orbital densities are projected along the direction of the wire by integrating out the other two dimensions. The geometric structure of the nanowire is shown on top to the same scale as the orbitals.

is facilitated preferentially by holes, rather than electrons, except for the highest energy excitation V. This is because the VB states of the metallic dot are in better resonance with the occupied states of the dye. Excitation V generates both hole and electron conductivity simultaneously. This excitation of porphyrin promotes an electron from HOMO to LUMO+1, Figure 3a. HOMO of porphyrin is close in energy to HOMO-2 of the cluster, while LUMO+1 of porphyrin is in resonance with a CB state on the cluster as well as an unoccupied state on the benzene bridge. Additionally, porphyrin's LUMO+1 has significant density on the sulfur atoms, contributing to the electron-mediated conductivity of excitation V. Electron conductivity is negligible in all other cases, and charge transport generated by photoexcitations I−IV is mediated by holes.

The conductivity of the nanowire depends strongly on the overlap of the charge carrying orbitals localized on the molecule and the cluster. The overlap determines the magnitude of the matrix element of the current operator $\langle j \rangle$, eq 8. The matrix element is maximized, if the donor and acceptor orbitals are delocalized between the molecule and the cluster. For example, the hole orbital participating in porphyrin excitation IV is delocalized onto the cluster more strongly than the hole orbital involved in excitation II, as seen in Figure 4, compare parts b and a, respectively. The hole orbitals involved in excitation II overlap little, and the conductivity is low, Figure 3c. At the same time, the hole orbitals involved in excitation IV overlap more significantly, facilitating high conductivity. Electron orbitals play the dominant role in the charge transport associated with excitation V. Interestingly, in this case the orbitals localized on the molecule and the cluster do not overlap directly, Figure 4c. The transport occurs through an auxiliary orbital, which is localized on the bridging benzene group. The benzene orbital overlaps with the orbitals of the molecule and the cluster and promotes electron transfer between them. All three orbitals are essential for charge transport.

The conductivity of the nanowire is very low in the absence of photoexcitation, Figure 3d. In the DC limit, it drops by more than 10 orders of magnitude and below the floating-point precision. The ground state conducts only when strong voltage is applied. Noticeable conductivity appears at voltages above 0.7 eV per cell. In this regime of relatively large voltages the linear response formalism described in Section III may break down, and the results should be interpreted qualitatively rather than quantitatively.

Optical excitation of the porphyrin molecule promotes conductivity by generating electron and hole pairs that are far from equilibrium. The excited states relax back to the ground state by coupling to phonons. The electron−phonon relaxation decreases the conductivity and heats up the system. The relaxation process should be particularly efficient inside the gold cluster, due to its quasicontinuous set of energy levels. Investigation of the energy relaxation requires a different set of theoretical techniques and can be performed, for instance, in time-domain and at the atomistic level by using nonadiabatic molecular dynamics.[45,78−80] To compensate for the relaxation and maintain high conductivity, optical pumping can be applied continuously during the whole time that the composite wire must conduct. In parallel, the heat generated by the electron−phonon energy transfer must be efficiently dissipated by coupling to the environment, including the DNA and a solvent or another medium. Even though fast electron−phonon relaxation causes rapid heating and loss of conductivity, it can be exploited to minimize the optical response time of the nanowire. Nanowire's conductivity increases from zero to a finite value nearly instantaneously on the time scale of an optical laser pulse. The conductivity decays back to zero on the time scale of electron−phonon relaxation. Thus, efficient relaxation facilitates fast optical switching of the conductivity of the DNA-templated gold−porphyrin nanowire.

VI. Conclusions

We considered a DNA-templated nanowire composed of an infinite periodic chain of gold clusters and porphyrin linkers. The electrical conductivity of the chain was investigated as a function of frequency of the applied electric field. Both ground state conductivity and its enhancement by a range of optical excitations of the porphyrin were studied. Porphyrin excitations were found extremely important for achieving good conductivity, because they generated charge carriers in the resonant states of the molecule and the cluster. Different optical transitions resulted in different conductivity, depending on the energetic proximity of the photoexcited molecular states to the electronic states of the gold cluster, as well as on the localization and overlap of the corresponding orbitals.

A small electric field applied along the composite nanowire initiates the following processes. A hole formed in an initially occupied orbital of the porphyrin by the photoexcitation transfers to the VB of the gold cluster, propagating in the direction of the applied field. An electron promoted to an

unoccupied orbital of the molecule flows in the direction opposite to the applied field and transfers to the CB of the cluster. By studying the efficiency of the carrier transport as a function of the optical excitation energy, we found specific molecular excitations that provide best conductivity. Generally, higher energy excitations yield better conductivity. The overlap of the donor and acceptor orbitals involved in the charge transport determine finer details of the conduction process and alter the general trend. Charge transport in the current system is facilitated primarily by holes, rather than electrons, as determined by the relative energies of the occupied and vacant states of the molecule and the cluster.

Electron−phonon interactions[78−80] inside the metal cluster result in energy relaxation and heating. Electrons and holes decay to the gold cluster states that are far away in energy from the molecular states. Optical pumping can be used to compensate for the relaxation, if applied continuously during the whole time that the composite wire is expected to conduct.[70] The electron−phonon relaxation time determines the response time of the nanowire, in the cases when fast optical control of the nanowire conductivity is desired.

Here we focused on conductivity along DNA. Recently, local scanning probes were applied to investigate DNA structure and sequence, generating tunneling currents across DNA chains.[81−84] Similar probes can be applied to the DNA−Au composites, and the methods presented here can be used to study the local tunneling currents.

The design of the optically gated quantum wire investigated in the present work carries two main advantages. Molecular interactions between the DNA, the gold cluster, the porphyrin, and the bridge promote self-assembly of the wire on the subnanometer scale. The nanowire has low latency time and can be optically switched on a picosecond time scale, as determined by the expected rapid recombination of electrons and holes inside the metal cluster. The reported study is supported by the available experimental data and provides further guidelines for the design of self-assembling molecular electronics units of nanometer and subnanometer sizes.

Acknowledgment. The funding was provided by grants from NSF CHE-0701517, DOE DE-FG02-05ER15755 and ACS-PRF 46772-AC6 to O.V.P. Work at Los Alamos was supported by DOE.

Supporting Information Available: Atomic coordinates of the gold-porphyrin nanowire. This material is available free of charge via the Internet at http://pubs.acs.org.

References and Notes

(1) Alivisatos, A. P. *Nature* **1996**, *382*, 609.
(2) Schatz, G. C. *Proc. Natl. Acad. Sci. U.S.A.* **2007**, *104*, 6885.
(3) Wong, K. L. *Science* **2007**, *315*, 1391.
(4) McCullagh, M. *J. Phys. Chem. B* **2008**, *112*, 10388.
(5) Alivisatos, A. P. *Science* **1996**, *271*, 933.
(6) Bawendi, M. G.; Steigerwald, M. L.; Brus, L. E. *Annu. Rev. Phys. Chem.* **1990**, *41*, 477.
(7) Tolbert, S. H.; Alivisatos, A. P. *Annu. Rev. Phys. Chem.* **1995**, *46*, 595.
(8) Waugh, F. R. *Phys. Rev. Lett.* **1995**, *75*, 705.
(9) Murray, C. B.; Norris, D. J.; Bawendi, M. G. *J. Am. Chem. Soc.* **1993**, *115*, 8706.
(10) Littau, K. A. *J. Phys. Chem.* **1993**, *97*, 1224.
(11) Mirkin, C. A.; Letsinger, R. L.; Mucic, R. C.; Storhoff, J. J. *Nature* **1996**, *382*, 607.
(12) Rosi, N. L.; Mirkin, C. A. *Chem. Rev.* **2005**, *105*, 1547.
(13) Seferos, D. S. *J. Am. Chem. Soc.* **2007**, *129*, 15477.
(14) Rosi, N. L. *Science* **2006**, *312*, 1027.
(15) Zheng, J. *Biophys. J.* **2008**, *95*, 3340.
(16) Seeman, N. *Nature* **2003**, *421*, 427.
(17) Jin, R. *J. Am. Chem. Soc.* **2003**, *125*, 1643.
(18) Park, S. *J. Phys. Chem. B* **2006**, *110*, 12673.
(19) Zhang, L.; Long, H.; Schatz, G. C.; Lewis, F. D. *Org. Biomol. Chem.* **2007**, *5*, 450.
(20) Park, S. Y.; Gibbs-Davis, J. M.; Nguyen, S. T.; Schatz, G. C. *J. Phys. Chem. B* **2007**, *111*, 8785.
(21) Park, S. Y. *Nature* **2008**, *451*, 553.
(22) Balzani, V.; Scandola, F. *Supramolecular Photochemistry*; Horwood: Chichester, U.K., 1991.
(23) Barth, J. V. *Annu. Rev. Phys. Chem.* **2007**, *58*, 375.
(24) Kilin, D. S.; Prezhdo, O. V.; Xia, Y. N. *Chem. Phys. Lett.* **2008**, *458*, 113.
(25) Maeda, Y. *J. Vac. Sci. Technol. B* **1999**, *17*, 494.
(26) Le, J. *Nano Lett.* **2004**, *4*, 2343.
(27) Sharma, J. *Angew. Chem., Int. Ed.* **2006**, *45*, 730.
(28) Nitzan, A.; Ratner, M. A. *Science* **2003**, *300*, 1384.
(29) Tagami, K.; Tsukada, M.; Matsumoto, T.; Kawai, T. *Phys. Rev. B* **2003**, *67*, 245324.
(30) Thanopulos, I.; Paspalakis, E. *Phys. Rev. B* **2007**, *76*, 035317.
(31) Wu, S. W.; Ogawa, N.; Ho, W. *Science* **2006**, *312*, 1362.
(32) Tsunashima, R. *Appl. Phys. Lett.* **2008**, *93*, 173102.
(33) Balbuena, P.; Derosa, P.; Seminario, J. *J. Phys. Chem. B* **1999**, *103*, 2830.
(34) Balbuena, P. B. *J. Phys. Chem. B* **2006**, *110*, 17452.
(35) Agapito, L. A.; Bautista, E. J.; Seminario, J. M. *Phys. Rev. B* **2007**, *76*, 115316.
(36) Habenicht, B. F.; Kalugin, O. N.; Prezhdo, O. V. *Nano Lett.* **2008**, *8*, 2510.
(37) Hohenberg, P.; Kohn, W. *Phys. Rev. B* **1964**, *3*, 864.
(38) Marques, M. A. L.; Gross, E. K. U. *Annu. Rev. Phys. Chem.* **2004**, *55*, 427.
(39) Hafner, J. *J. Comput. Chem.* **2008**, *29*, 2044.
(40) Janak, J. F. *Phys. Rev. B* **1978**, *18*, 7165.
(41) Melnikov, D. V.; Chelikowsky, J. R. *Phys. Rev. B* **2004**, *69*, 113305.
(42) Runge, E.; Gross, E. K. U. *Phys. Rev. Lett.* **1984**, *52*, 997.
(43) Aikens, C. M.; Schatz, G. C. *J. Phys. Chem. A* **2006**, *110*, 13317.
(44) Kosov, D. *J. Chem. Phys.* **2003**, *119*, 1.
(45) Craig, C. F.; Duncan, W. R.; Prezhdo, O. V. *Phys. Rev. Lett.* **2005**, *95*, 163001.
(46) Kilin, D. S. et al. *J. Photochem. Photobiol. A* **2007**, *190*, 342.
(47) Prezhdo, O. V.; Kindt, J. T.; Tully, J. C. *J. Chem. Phys.* **1999**, *111*, 7818.
(48) Wu, Q.; Van Voorhis, T. *Phys. Rev. A* **2005**, *72*, 024502.
(49) Hong, G.; Rosta, E.; Warshel, A. *J. Phys. Chem. B* **2006**, *110*, 19570.
(50) Kilina, S. et al. *J. Phys. Chem. C*, **2007**, *111*, 14541.
(51) Gelin, M. F.; Kosov, D. S. *Phys. Rev. E* **2008**, *78*, 011116.
(52) Li, Z.; Kosov, D. S. *J. Phys. Chem. B* **2006**, *110*, 19116.
(53) Nitzan, A. *Annu. Rev. Phys. Chem.* **2001**, *52*, 681.
(54) Ashcroft, N. W.; Mermin, N. D. *Solid State Physics*; Saunders: New York, 1976.
(55) Smith, R. A. *Semiconductors*; University Press: Cambridge, UK, 1959.
(56) Vojta, T.; Epperlein, F.; Schreiber, M. *Phys. Rev. Lett.* **1998**, *81*, 4212.
(57) Greenwood, D. A. *Proc. R. Soc. London* **1958**, *71*, 585.
(58) Epperlein, F. et al. *Phys. B*, **2001**, *296*, 52.
(59) Shi, J.; Xie, X. *Phys. Rev. Lett.* **2003**, *91*, 086801.
(60) Yaliraki, S. *J. Chem. Phys.* **1999**, *111*, 6997.
(61) Landauer, R. *Philos. Mag.* **1970**, *21*, 863.
(62) Staykov, A.; Nozaki, D.; Yoshizawa, K. *J. Phys. Chem. C* **2007**, *111*, 3517.
(63) Datta, S. *Electronic transport in mesoscopic systems*; University Press: Cambridge, UK, 1995).
(64) Brandbyge, M. *Phys. Rev. B* **2002**, *65*, 165401.
(65) Taylor, J.; Guo, H.; Wang, J. *Phys. Rev. B* **2001**, *63*, 245407.
(66) Datta, S. *Phys. Rev. Lett.* **1997**, *79*, 2530.
(67) Girard, Y.; Kondo, M.; Yoshizawa, K. *Chem. Phys.* **2006**, *327*, 77.
(68) Yanov, I.; Kholod, Y.; Leszczynski, J.; Palacios, J. J. *Chem. Phys. Lett.* **2007**, *445*, 238.
(69) Martin, R. M. In *Electronic Structure: Basic Theory and Practical Methods*; Cambridge University Press: Cambridge, MA, 2004; Chapters 12 and 13.
(70) Kilin, D.; Micha, D. A. *Chem. Phys. Lett.* **2008**, *461*, 266.
(71) Kamisaka, H.; Kilina, S. V.; Yamashita, K.; Prezhdo, O. V. *Nano Lett.* **2006**, *6*, 2295.
(72) Kara, A.; Rahman, T. S. *Phys. Rev. Lett.* **1998**, *81*, 1453.
(73) Kresse, G.; Furtmüller, J. *Phys. Rev. B* **1996**, *54*, 11169.
(74) Vanderbilt, D. *Phys. Rev. B* **1990**, *41*, 7892.
(75) Perdew, J. P.; Wang, Y. *Phys. Rev. B* **1992**, *45*, 13244.
(76) Gouterman, M. *J. Mol. Spectrosc.* **1961**, *6*, 138.

(77) Aikens, C. M.; Li, S.-Z.; Schatz, G. C. *J. Phys. Chem. C* **2008**, *112*, 11272.
(78) Habenicht, B. F.; Craig, C. F.; Prezhdo, O. V. *Phys. Rev. Lett.* **2006**, *96*, 187401.
(79) Kilina, S. V.; Kilin, D. S.; Craig, C. F.; Prezhdo, O. V. *J. Phys. Chem. C* **2007**, *111*, 4871.
(80) Habenicht, B. F.; Prezhdo, O. V. *Phys. Rev. Lett.* **2008**, *100*, 197402.
(81) Yarotski, D. et al. *Nano Lett.*, **2009**, *9*, 12.
(82) Takami, T.; Tanaka, H.; Kawai, T. *Surf. Sci.* **2008**, *602*, L39.
(83) Shapir, E. *Nat. Mater.* **2008**, *7*, 68.
(84) Porath, D.; Bezryadin, A.; de Vries, S.; Dekker, C. *Nature* **2000**, *403*, 635.

JP811169C